

EFFECTS OF ENVIRONMENT AND COMPLEX LOAD HISTORY ON FATIGUE LIFE

A symposium
presented at the
Fall Meeting
AMERICAN SOCIETY FOR
TESTING AND MATERIALS
Atlanta, Ga., 29 September-4 October, 1968

ASTM SPECIAL TECHNICAL PUBLICATION 462

List Price \$22.00



AMERICAN SOCIETY FOR TESTING AND MATERIALS
1916 Race Street, Philadelphia, Pa. 19103

© BY AMERICAN SOCIETY FOR TESTING AND MATERIALS 1970

Library of Congress Catalog Card Number: 73-89676

SBN 8031-0050-7

NOTE

The Society is not responsible, as a body,
for the statements and opinions
advanced in this publication.

Foreword

The Symposium on Effects of Environment and Complex Load History on Fatigue Life was presented at the Fall Meeting of ASTM held in Atlanta, Ga., 29 September-4 October, 1968. Committee E-9 on Fatigue sponsored the symposium. M. S. Rosenfeld, U.S. Naval Air Engineering Center, was responsible for the session on Cumulative Damage and Life Estimation. S. R. Swanson, MTS Systems, was responsible for the session on Fatigue Under Random Loads. D. W. Hoeppner, Battelle Memorial Institute and R. I. Stephens, University of Iowa, were responsible for the two sessions on Influence of Environment on Fatigue.

Related ASTM Publications

Structural Fatigue in Aircraft, STP 404 (1966), \$18.50

Fatigue Crack Propagation, STP 415 (1967), \$30.00

**Low Cycle Fatigue Bibliographic Survey, STP 449
(1968), Microfiche, \$3.00**

**Fatigue at High Temperature, STP 459 (1969),
\$11.25**

Introduction

In keeping with a well established precedent, Committee E-9 on Fatigue again sponsored a triennial symposium on aircraft structural fatigue problems at the Fall Meeting held in Atlanta, Ga., 29 Sept.-4 Oct. 1968.

Previous symposia have concentrated on the basic mechanism of fatigue, the effects of stress concentrations, and the behavior of full-scale structural assemblies and components under simulated service loadings.

This symposium was divided into three broad categories: (1) cumulative damage; (2) random load effects; and (3) the effects of corrosive environments.

In general, the papers in the first two categories approach the basic problem of life estimation in a more rational manner than heretofore. The papers on the effects of corrosive environments reflect the current concern with the superposition of environmental simulation on the fatigue problem.

M. S. Rosenfeld

Research Aerospace Engineer,
Aero Structures Department,
Naval Air Development
Center; symposium chairman.

Contents

Introduction.....	vii
The Effect of Stress Ratio During Crack Propagation and Fatigue for 2024-T3 and 7075-T6 Aluminum—K. WALKER.....	1
Constant Amplitude and Cumulative Damage Fatigue Tests on Bailey Bridges—D. WEBBER.....	15
Cumulative Damage Analysis in Structural Fatigue—L. F. IMPELLIZZERI.....	40
Discussion.....	69
Laboratory Simulation of Structural Fatigue Behavior—J. MORROW, R. M. WETZEL, AND T. H. TOPPER.....	74
Discussion.....	92
Effects of Mean Stress and Prestrain on Fatigue-Damage Summation— T. H. TOPPER AND B. I. SANDOR.....	93
Peak-Distribution Effects in Random-Load Fatigue—JENS TRAMPE BROCH... ..	105
Effects of Block Size, Stress Level, and Loading Sequence on Fatigue Char- acteristics of Aluminum-Alloy Box Beams—WILLIAM BREYAN.....	127
Fatigue Life of 2024-T3 Aluminum Alloy Under Narrow- and Broad-Band Random Loading—B. M. HILLBERRY.....	167
Comparison of Fatigue Lives Under Conventional Program Loading and Digital Random Loading—G. H. JACOBY.....	184
Effects of Notches and Saltwater Corrosion on the Flexural Fatigue Behavior of High-Strength Structural Alloys—R. C. SCHWAB AND E. J. CZYRYCA... ..	203
Effect of Oxygen and of Water Vapor on the Fatigue Life of Nickel at 300 C— H. H. SMITH AND P. SHAHINIAN.....	217
Tensile and Shear-Mode Cracking of Titanium Sheet in Air and in Salt Water—K. WALKER, S. PENDLEBERRY, AND R. MCELWEE.....	234
Evaluation of Methods to Alleviate Corrosion Fatigue in Type 135 Drill-Pipe Steel for Offshore-Drilling Applications—D. E. PETTIT, D. W. HOEPPNER, AND W. S. HYLER.....	241
The Influence of Salt Water on Fatigue-Crack Growth in High-Strength Structural Steels—T. W. CROOKER AND E. A. LANGE.....	258
Predicting Low-Cycle Fatigue Data for Low-Alloy Cast Steels—A. K. SCHMIEDER.....	272
Effect of Tempering Temperature on Fatigue-Crack Propagation in 4340 Steel—ALBERT A. ANCTL AND ERIC B. KULA.....	297
A New Apparatus for Investigating Friction and Metal-to-Metal Contact in Fretting Joints—W. D. MILESTONE.....	318

The Effect of Stress Ratio During Crack Propagation and Fatigue for 2024-T3 and 7075-T6 Aluminum

REFERENCE: Walker, K., "The Effect of Stress Ratio During Crack Propagation and Fatigue for 2024-T3 and 7075-T6 Aluminum," *Effects of Environment and Complex Load History on Fatigue Life, ASTM STP 462*, American Society for Testing and Materials, 1970, pp. 1-14.

ABSTRACT: An effective stress, $\bar{\sigma} = \sigma_{\max}^{1-m} \Delta \sigma^m$ where m is assumed to be a material constant, is shown to predict the effect of stress ratio on crack propagation and fatigue life for two aluminum alloys. Simple approximations of notch stress and strain using Neuber's notch rule are introduced to extend the predictions of stress-ratio effects to inelastic notch behavior.

KEY WORDS: stress ratio, fatigue, crack propagation, fracture mechanics, notch stress, aluminum alloys

Nomenclature

a	One half of total crack length, in.
K_f	Fatigue notch factor
K_T	Elastic notch factor
K_{\max}	Maximum stress-intensity parameter, $\gamma S_{\max} \sqrt{2a}$, ksi $\sqrt{\text{in.}}$
\bar{K}	Effective stress-intensity parameter, $\gamma \bar{S} \sqrt{2a}$, ksi $\sqrt{\text{in.}}$
$d(2a)/dN$	Crack-growth rate, micro-inches per cycle
N	Cycles of loading, crack growth; cycles to failure, fatigue life
R	Stress ratio, S_{\min}/S_{\max}
S_{\max}	Maximum stress, ksi
S_{\min}	Minimum stress, ksi
S_m	Mean stress, ksi
S_a	Alternating stress, one half of stress range ΔS , ksi
ΔS	Stress range, $(S_{\max} - S_{\min})$, ksi
\bar{S}	Effective stress, $S_{\max}^{1-m} \Delta S^m$, ksi

¹ Senior Research Scientist, Physical Sciences Laboratory, Lockheed-California Company, P.O. Box 551, Burbank, Calif. 91503.

γ	Width-correction factor
σ_{\max}	Maximum notch stress, ksi
e	Strain, in. per in.
$\Delta\sigma$	Stress range at notch, ksi
$\bar{\sigma}$	Notch effective stress, $\sigma_{\max}^{1-m} \Delta\sigma^m$, ksi
σ_1	Maximum notch stress for single-cycle loading, ksi
m	An exponent, assumed to have a single value for both crack propagation and fatigue life
n	An exponent

Introduction

This report brings together observations made from crack-propagation data and from fatigue data for two aluminum alloys. The purpose is twofold: first, to present a simple expression accounting for stress-ratio effects; and second, to illustrate that as far as stress-ratio effects are concerned, there is a close similarity between crack nucleation and crack propagation. Supporting evidence of fatigue-life data and crack-propagation data is shown for the effect of stress ratio. In order to extend the observations to notch fatigue, some simple approximations of notch stress and strain using Neuber's notch rule are introduced.

Crack Propagation

Brock and Schijve [1],² McMillan and Pelloux [2], and Erdogan [3] have concluded that the general equation relating stress to crack-growth rate and crack length is of the form:

$$\frac{d(2a)}{dN} = f[\gamma(S_{\max}\sqrt{2a})^c (\Delta S\sqrt{2a})^b] \dots\dots\dots (1)$$

This equation can be rewritten

$$\frac{d(2a)}{dN} = f\{\gamma(S_{\max}^{1-m})(\Delta S^m)\sqrt{2a}\}^n \dots\dots\dots (2)$$

where:

$$\begin{aligned} 1 - m &= c/(c + b) \\ m &= b/(c + b) \\ n &= c + b \end{aligned}$$

Since the product of the two stress terms in Eq 2 has the dimensions of stress, an effective stress can be defined.

$$\bar{S} = S_{\max}^{1-m} \Delta S^m = S_{\max}(1 - R)^m \dots\dots\dots (3)$$

² The italic numbers in brackets refer to the list of references appended to this paper.

And an equation for crack growth can be written in the form

$$\frac{d(2a)}{dN} = f(\gamma \bar{S} \sqrt{2a}) = f(\bar{\Delta}K) \dots \dots \dots (4)$$

Cracking-rate data for 2024-T3 and 7075-T6 aluminum [1] are shown in Fig. 1 using $\bar{\Delta}K$ as abscissa. Values of m used in computing $\bar{\Delta}K$ were de-

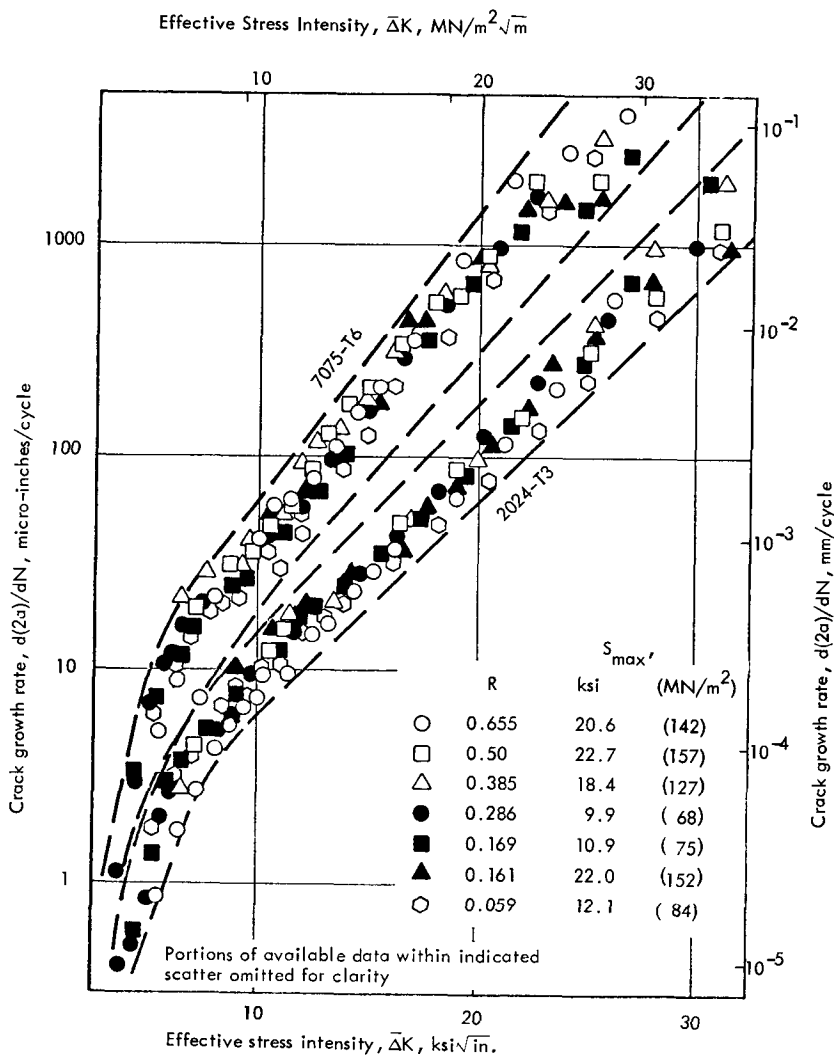


FIG. 1—Crack growth in 2024-T3 and 7075-T6.

terminated for best fit using available computer routines. The values of m used were 0.5 for 2024-T3 aluminum and 0.425 for 7075-T6 aluminum. According to Brock and Schijve [1], the crack rotation from a tensile to a shear mode of cracking for 2024-T3 occurred at a single cracking rate and thus at a single value of $\bar{\Delta}K$ (Fig. 2). This rotation of the crack is the result of a change in stress state from triaxial to biaxial near the crack tip [4]. At high values of $\bar{\Delta}K$ the accumulation of cyclic slip near the crack tip results in a relaxation of the triaxial stress state causing the principal shear stresses to change from 90- to 45-deg planes. The crack rotates to follow this change in orientation of the principal shear planes. Figure 2 shows that this rotation, and thus cumulative cyclic slip, is dependent on both maximum and alternating stresses in proportions given by \bar{S} .

Further evidence that local cyclic stress and strain near the crack tip vary with \bar{S} can be found by examining cracking-rate data from differing environments (Fig. 3) [5]. In Fig. 3, crack-growth rate is seen to be influenced by environment. However, the effect of stress ratio as accounted for by \bar{S} is independent of environment.

The data shown in Figs. 1-3 include only positive stress ratios. Fatigue cracks may close under compressive loading so that for these cases, dif-

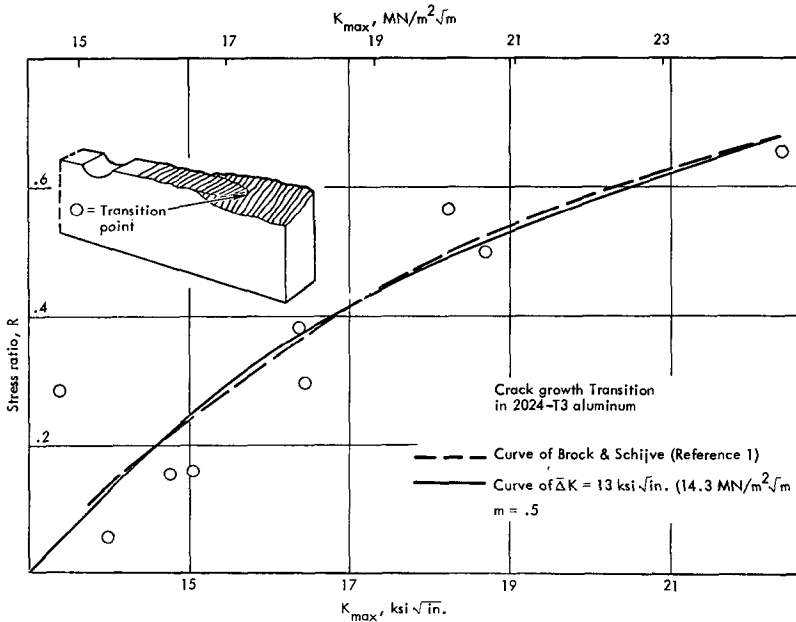


FIG. 2—Tensile to shear mode cracking transition, 2024-T3.

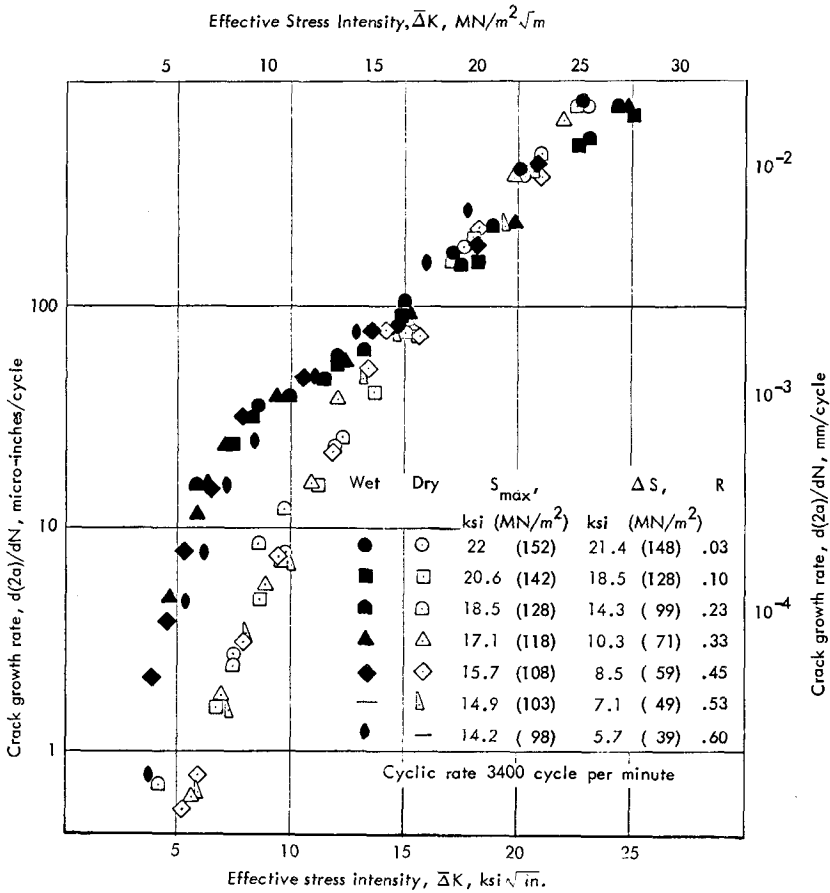


FIG. 3—Crack growth in dry and wet air, 7075-T6.

ferences between local tensile and compressive stress distribution near the crack must be determined. Thus, possible use of the effective stress for crack growth with compressive loading requires further study.

Fatigue of Unnotched Coupons and of Notched Coupons with Elastic Notch Stress-Strain

During crack propagation, cyclic slip and the material state at a level sensitive to corrosive environments are related to both maximum and alternating stresses in the ratio given by \bar{S} . That this same ratio may apply also to fatigue data can now be considered. Figures 4 and 5 show unnotched fatigue data [6]. The values of m used in computing the stress ordinate are

those previously determined from the crack-growth data. Figures 4 and 5 show that the effect of stress ratio for fatigue life of unnotched coupons is approximately the same as that for crack propagation.

The elastic limit for sharply notched round specimens is between 2 and 3 times that for notched sheet specimens due to the triaxial state of stress.

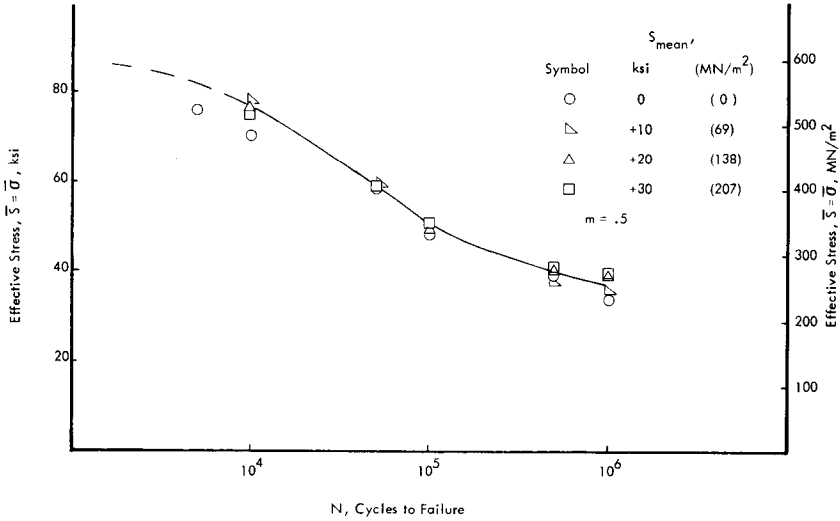


FIG. 4—Unnotched fatigue, 2024-T3.

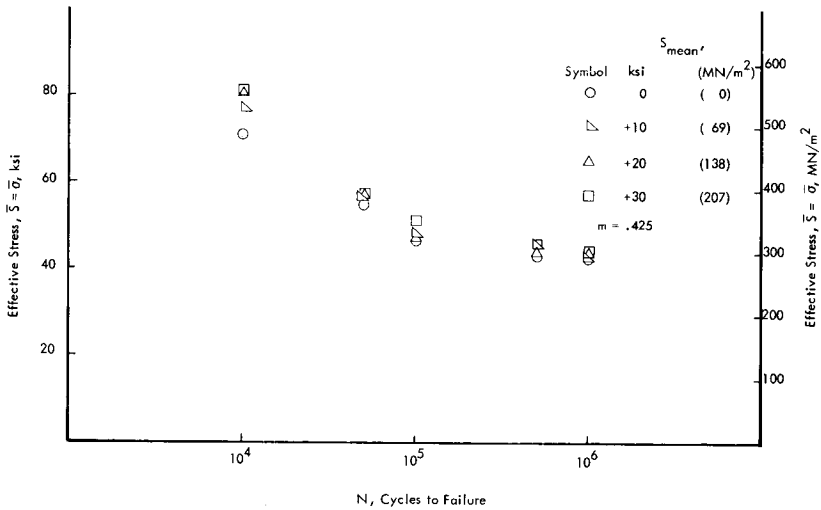


FIG. 5—Unnotched fatigue, 7075-T6.

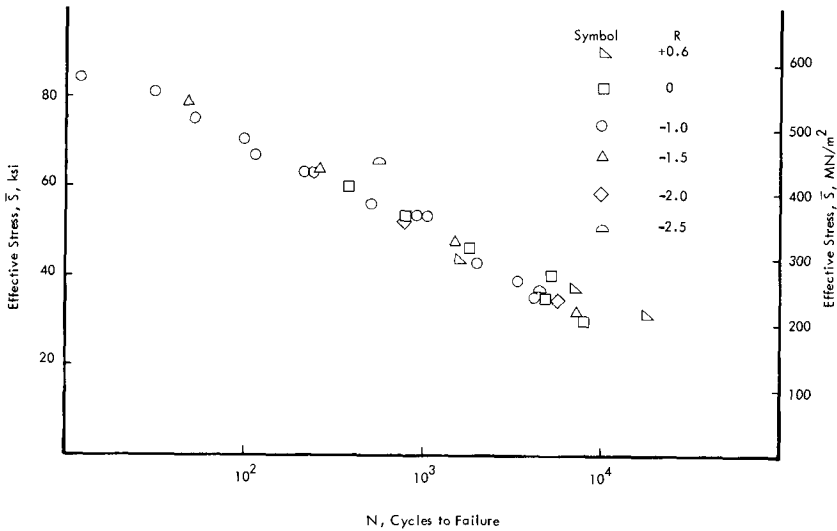


FIG. 6—Fatigue life for $K_T = 5$ notched round specimens, 2024-T3.

Inelastic strains are also suppressed. For elastic notch stress-strain the nominal effective stress \bar{S} is proportional to the notch effective stress $\bar{\sigma}$. Figures 6 and 7 [7] show fatigue data for $K_T = 5$ for notched round specimens. Reasonable correlation is obtained for stress ratios between -2.5 and $+0.6$, using \bar{S} as ordinate.

Fatigue of Notched Coupons with Inelastic Notch Stress-Strain

Whenever notch stresses are inelastic, the stress ratio locally at the site of potential fatigue damage is not the same as that remote from the notch. Effective stress, \bar{S} , is not proportional to $\bar{\sigma}$. Studies of notch fatigue [8, 9] provide information for simple approximations to relate \bar{S} to $\bar{\sigma}$ for 2024-T3. Topper et al [8] and Wetzel [9] use the relationship for true notch stress and strain proposed by Neuber [10].

$$K_T = \sqrt{K_\sigma K_\epsilon} \dots \dots \dots (5)$$

Whenever the stress, remote from the stress concentration, is elastic, Eq 5 becomes

$$K_T = \sqrt{\frac{\sigma}{S} \times \frac{eE}{S}}$$

and can be rewritten

$$\frac{(K_T S)^2}{E} = \sigma e \dots \dots \dots (6)$$

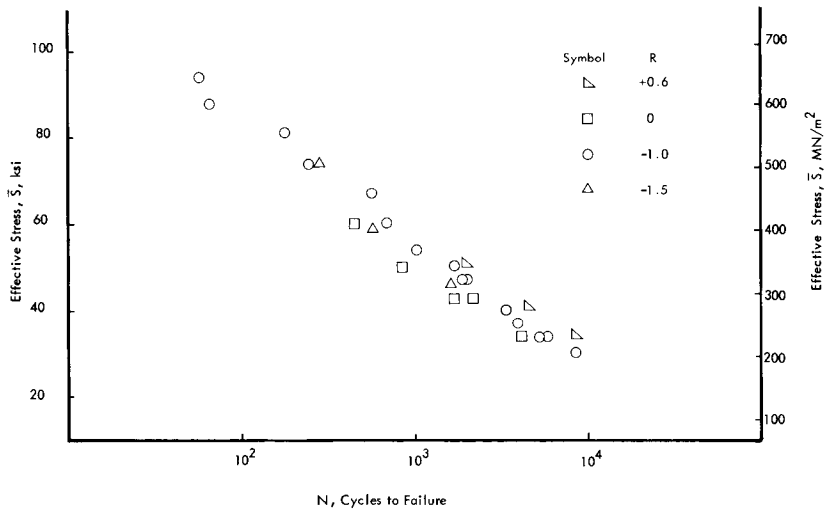


FIG. 7—Fatigue life for $K_T = 5$ notched round specimens, 7075-T6.

The fatigue notch factor K_f is substituted for the elastic stress-concentration factor K_T [8, 9].

$$\frac{(K_f S)^2}{E} = \sigma e \dots \dots \dots (7)$$

Equation 7 can be used to superimpose curves of constant $(K_f S)^2/E$ on cyclic or monotonic stress-strain curves to obtain the solution of Eq 7 which is also compatible with the material stress-strain properties [9]. This procedure is used in Fig. 8.

For $R = -1$, according to Topper et al [8] and Wetzel [9], notch stress is approximately defined by Neuber's notch rule and the cyclic stress-strain curve (Fig. 8a). When the stress range is relatively small, the maximum notch stress is approximately defined by Neuber's notch rule and the monotonic stress-strain curve. If some additional approximations are introduced, Figs. 8b and c may be constructed. For the case $R = 0$, the notch-stress range is primarily elastic and approximately equal to $K_f \Delta S$ (Fig. 8b). The limit of $K_f \Delta S$ for which the stress range remains elastic can be approximated by $K_f \Delta S \geq 2\sigma_1$ (Fig. 8b). Whenever $K_f \Delta S$ is between $2\sigma_1$, and $2K_f S_{max}$, a simple proportionate estimate is assumed (Fig. 8c). In Fig. 8c, the cyclic stress-strain curve was shifted proportionately, as shown, to obtain new intersections with the Neuber curve. This method was chosen for its expedience while examining graphic displays of the type of Fig. 8c rather than for theoretical reasons. Any reasonable method of interpolation will give approximately the same results.

Typical calculations for the notch effective stress using the approximations of Fig. 8 are shown in Fig. 9. The relationship between \bar{S} and $\bar{\sigma}$ determined in the manner of Fig. 9 can be used to predict the effect of stress ratio on the fatigue life of notched coupons with inelastic notch behavior.

A Modified Goodman Diagram

From several calculations of the type illustrated by Fig. 9, Fig. 10 can be constructed. Values of $\bar{\sigma}$ are plotted using alternating and mean-stress

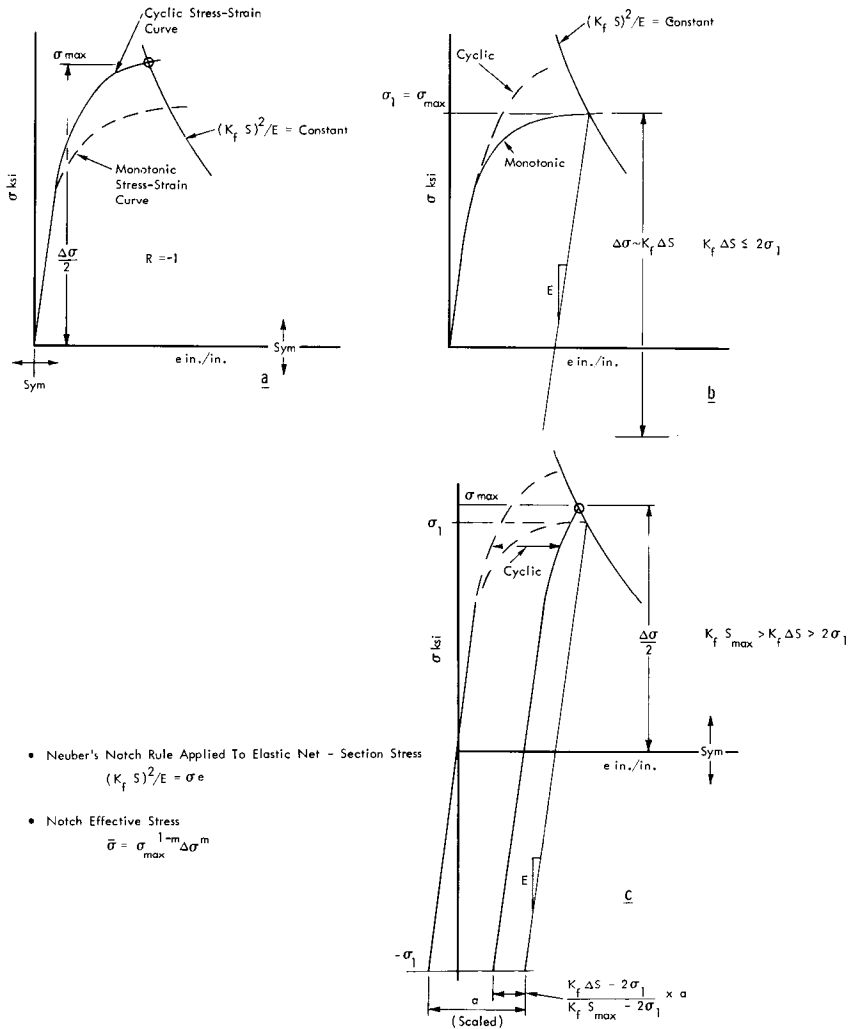


FIG. 8—Approximations for notch effective stress.

$K_f S_{max}$ ksi (MN/m ²)	$K_f \Delta S$ ksi (MN/m ²)	σ_{max} ksi (MN/m ²)	$\bar{\sigma}^*$ ksi (MN/m ²)
87.5 (605)	5 (48)	53 (366)	16 (110)
85 (586)	10 (69)	53	23 (159)
80 (551)	20 (138)	53	33 (228)
75 (518)	30 (207)	53	40 (276)
70 (483)	40 (276)	53	46 (318)
65 (449)	50 (345)	53	52 (359)
60 (414)	60 (414)	53	56 (386)
50 (345)	70 (483)	53	61 (421)
50 (345)	80 (552)	53	65 (449)
45 (311)	90 (621)	53	69 (476)
40 (276)	100 (690)	53	72 (496)
37 (255)	106 (730)	53	75 (417)
32 (221)	116 (180)	55 (379)	77.5 (435)
24 (166)	132 (910)	59 (407)	83 (573)
16 (110)	148 (1020)	62 (428)	87 (600)
8 (55)	164 (1130)	66 (455)	93 (642)
0 (0)	180 (1240)	67 (463)	95 (655)

* For $K_f \Delta S > 106$ ksi,

notch mean stress ~ 0
 $\bar{\sigma} = (\sigma_{max})^{1/2} (2 \sigma_{max})^{1/2} = \sigma_{max} \sqrt{2}$

For $K_f \Delta S < 106$ ksi

$\Delta \sigma \sim K_f \Delta S$

$\bar{\sigma} = (\sigma_{max})^{1/2} (K_f \Delta S)^{1/2}$

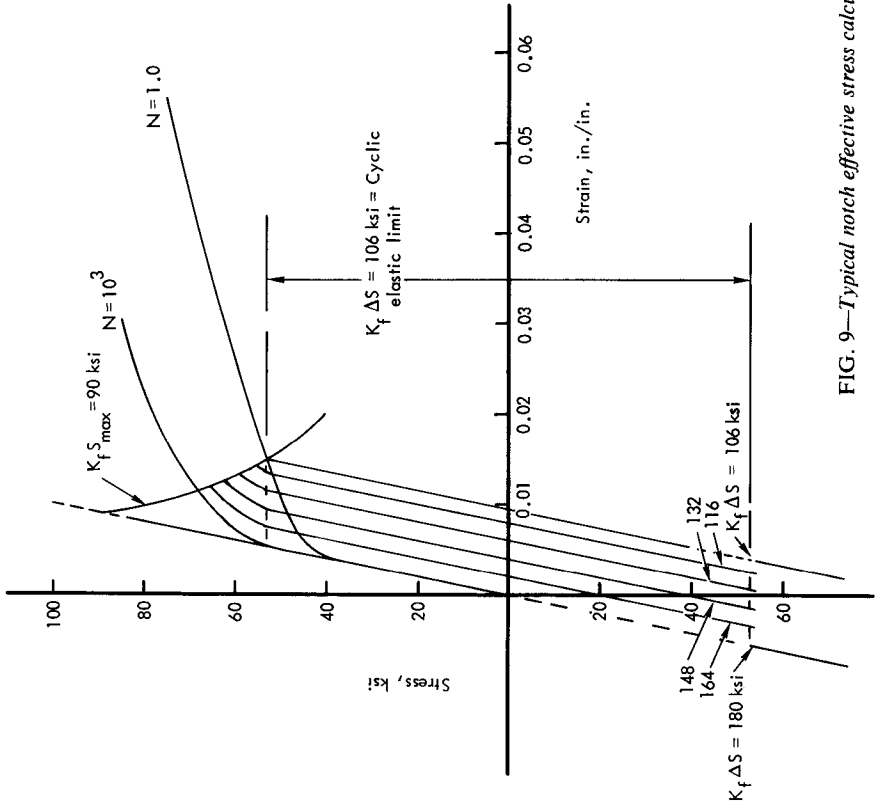


FIG. 9—Typical notch effective stress calculations, 2024-T3.

coordinates. Lines of constant $\bar{\sigma}$ are mapped onto the figure. Values of $\bar{\sigma}$ for negative mean stress were estimated by assuming stress-strain behavior as symmetric about zero stress. The mapped lines of constant $\bar{\sigma}$ are related to fatigue life using unnotched coupon fatigue data where $\bar{S} \sim \bar{\sigma}$ (Fig. 4). Figure 10 is based on approximations not yet fully substantiated by test.

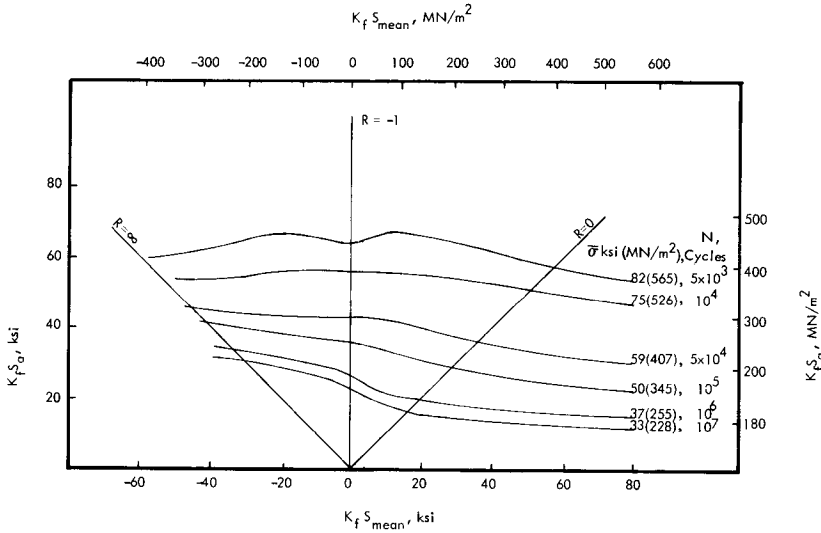


FIG. 10—Modified Goodman diagram derived from unnotched coupon data, 2024-T3.

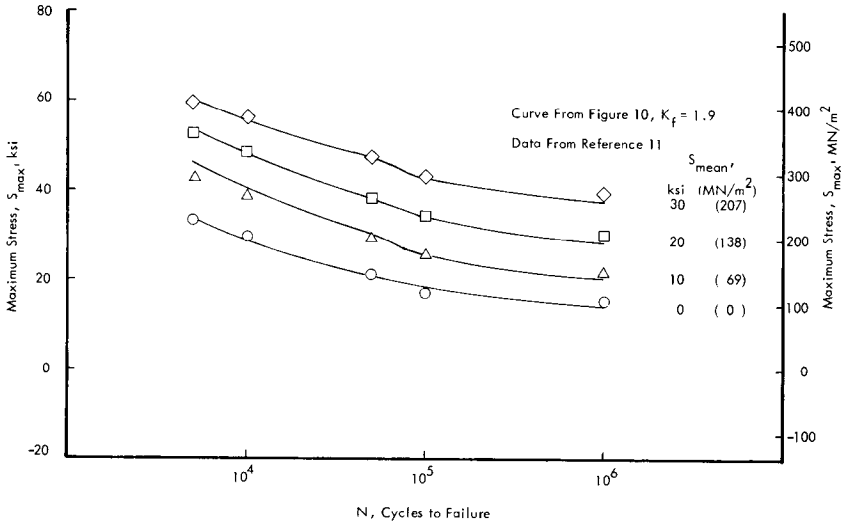


FIG. 11—Fatigue life for $K_T = 2$ sheet coupons, 2024-T3.